

# Kinetics and Mechanism of the Atmospheric Oxidation of Tertiary Amyl Methyl Ether

D. F. SMITH, C. D. MCIVER, and T. E. KLEINDIENST

*ManTech Environmental Sciences, P.O. Box 12313, Research Triangle Park, North Carolina 27709*

## Abstract

Tertiary-amyl methyl ether (TAME) is proposed for use as an additive to increase the oxygen content of gasoline as stipulated in the 1990 Clean Air Amendments. The present experiments have been performed to examine the kinetics and mechanisms of the atmospheric removal of TAME. The kinetics of the reaction of OH with TAME was examined by using a relative rate technique in which photolysis of methyl nitrite or nitrous acid was used as the source of OH. The OH rate constant for TAME and two major products (*t*-amyl formate and methyl acetate) were measured and yields for ten products were determined as primary products from the reaction.

Values determined for the rate constants for the reaction with OH were  $5.48 \times 10^{-12}$  (TAME),  $1.75 \times 10^{-12}$  (*t*-amyl formate), and  $3.85 \times 10^{-13} \text{ cm}^3 \text{ molec}^{-1} \text{ s}^{-1}$  (methyl acetate) at  $298 \pm 2 \text{ K}$ . The primary products (with corrected yields where required) from the OH + TAME that have been observed include (1) *t*-amyl formate (0.366), methyl acetate (0.349), acetaldehyde (0.43, corrected), acetone (0.036), formaldehyde (0.549), *t*-amyl alcohol (0.026), 3-methoxy-3-methyl-butanal (0.044, corrected), *t*-amyloxy methyl nitrate (0.029), 3-methoxy-3-methyl-2-butyl nitrate (0.010), and 2-methoxy-2-methyl butyl nitrate (0.004). Mechanisms leading to these products involve OH abstraction from each of the four different hydrogen atoms of TAME. © 1995 John Wiley & Sons, Inc.

## Introduction

Several ethers are currently being considered for use in the United States as an additive in gasoline. The branched ethers, in particular, are being adopted as important components in reformulated gasolines currently being developed by major petroleum companies. From a health perspective, the use of these compounds in large quantities, as in automotive fuels, demands that their atmospheric lifetime and the lifetimes of the photochemical decomposition products be accurately known. In addition, the reaction products from the atmospheric oxidation of these compounds must be known for inclusion in chemical kinetics models. Tertiary-amyl methyl ether (TAME;  $(\text{CH}_3\text{CH}_2)(\text{CH}_3)_2\text{C}-\text{O}-\text{CH}_3$ ) is one such ether under consideration that has the advantage of lower volatility than lower molecular weight ethers such as MTBE.

Previous studies which have been conducted for this compound have been relatively sparse. Wallington et al. [1] measured an OH rate constant for TAME ( $7.91 \times 10^{-12} \text{ cm}^3 \text{ molec}^{-1} \text{ s}^{-1}$ ) and other ethers using a flash-photolysis resonance fluorescence technique. In a recent publication, Wallington et al. [2] have remeasured the OH rate constant for TAME using both flash photolysis and relative rate methods. At 296 K, the flash photolysis method yielded a result of  $5.5 \times 10^{-12} \text{ cm}^3 \text{ molec}^{-1} \text{ s}^{-1}$  while the relative rate method gave comparable results using three different reference compounds. These values are about 30% lower than the earlier reported

value. However, there are no publications reporting product or product yields from the photooxidation of TAME.

In the work presented in this article, the rate constant for OH with TAME was also measured by a relative rate method [3] using the photolysis of  $\text{CH}_3\text{ONO}$  as the source of OH. Relative rate measurements have also been performed for the reaction rate of OH + two of the major products, *t*-amyl formate (TAF) and methyl acetate. No previous measurements for the TAF have been reported while values differing by a factor of 2 have been reported for methyl acetate [4,5]. The product distribution from the reaction of OH with TAME was also studied by irradiation mixtures of TAME with  $\text{CH}_3\text{ONO}$  or HONO in the presence of excess NO in air. From these data, product identifications and yields are established and branching ratios for OH attack on the methoxy side of TAME vs. the *t*-amyl side of the molecule can be evaluated.

## Experimental Methods

### *Apparatus and Materials*

Experiments to measure rate constants and yields of the reaction products of OH with TAME were conducted with an apparatus similar to that which has been described previously [6]. Irradiations were performed in 200-L reaction chambers constructed of 50- $\mu\text{m}$  Teflon film. The irradiation chamber consisted of a reaction chamber with two light banks, each with a mixture of eight florescent bulbs spanning the range of 300–450 nm. The  $\text{NO}_2$  photolysis rate of this system is  $0.46 \text{ min}^{-1}$ . A 50 L/min fan was used to cool the inside of the chamber, maintaining a reaction temperature of approximately 298 K. Reactants were introduced and samples were withdrawn through a 6.4-mm Swagelok fitting affixed to the chamber. Purified air from a pure air generator (Balston, Inc., Haverhill, Massachusetts) was added as a diluent to the reaction chambers through a 0–10 L/min mass flow meter (Tylan General, Inc., Torrance, California). The flow meter was calibrated against a dry test meter which was cross-calibrated against an NIST-traceable standard. The filler system was equipped with a syringe injection port facilitating the injection of both liquid and gaseous reactants into the chambers in a flowing airstream. All reactant mixtures and calibration standards were generated by this system.

Reactant and product concentrations were measured by using GC, high-performance liquid chromatography (HPLC), or gas chromatography/mass spectroscopy (GC/MS). For GC analysis of the gas samples, the precision and accuracy of the measurements were largely dependent on the integrity of the injection system. Gas samples for GC analysis were collected and injected by using a cryogenic sampling system which has been described in detail elsewhere [7]. Briefly, the cryogenic sampling inlet system consisted of the heated rotary valve with a Hastelloy C sample loop, a heated inlet line, and a Restek Silco-steel<sup>TM</sup> (Restek Corp., Bellefonte, Pennsylvania) coated sample loop. For the cryogenic system, collection volumes drawn through the inlet system were measured with a 0–100  $\text{cm}^3/\text{min}$  mass flow controller. The heated inlet line employed a 3.2-mm stainless steel three-way valve to flush the loop with carrier gas prior to injection. Liquid nitrogen was used for cooling and maintaining the sample loop at  $-180^\circ\text{C}$ , and three 200W cartridge heaters were used for heating the sample loop. The loop temperature was controlled by a programmable temperature controller (Omega Engineering, Inc., Stamford, Connecticut). Samples were collected for a fixed

period of time in the loop. After collection, samples were injected onto the GC column by rapidly and reproducibly raising the loop temperature to 260°C. This injection system was used in both kinetics experiments and product yield experiments.

Analyses of the organic components before and during the irradiation were performed by using a Hewlett-Packard (HP) 5890 Series II GC equipped with a flame ionization detector (FID), and ECD and an MS-DOS data acquisition system with Chrom Perfect Direct™ (Justice Innovations Inc., Palo Alto, California) chromatographic software. The compounds were separated by either: (1) HP-5 capillary column (0.32-mm i.d., 50-m-length, and 1- $\mu$ m film thickness); (2) an HP-5 megabore column (0.53-mm i.d., 30-m length, 2.65- $\mu$ m film thickness) coupled to a J&W DB-WAX (0.53-mm i.d., 15-m length, 1.0  $\mu$ m film thickness); or (3) a Restek RT<sub>x</sub>-200 (0.32-mm i.d., 30-m length, 1.0- $\mu$ m film thickness). Helium was used as the carrier gas, and the GC oven temperature was programmed according to the boiling points of the analytes detected.

Product identifications were performed with an HP-5971A mass selective detector (MSD) and/or a Bio-Rad GC Lightpipe Accessory attached to a Bio-Rad FTS 25 Fourier Transform Infrared Spectrometer. A deactivated fused silica transfer line (0.1-mm i.d.  $\times$  60 cm) was installed into the source of the MSD and connected to one side of a glass capillary "Y" splitter (Restek Corp.). The other side of the "Y" was connected to the FTIR lightpipe inlet using another section of deactivated fused silica transfer line (0.25-mm i.d.  $\times$  100 cm). The outlet from the lightpipe was connected to the GC/FID with deactivated fused silica transfer line (0.32-mm i.d.  $\times$  60 cm). The GC analytical column outlet is connected to the "Y" splitter inlet. The net effect is to split the column effluent  $\approx$ 2:1 to the FTIR:MS detectors for simultaneous analysis of the analyte peaks. The GC-FTIR was operated at an 8 cm<sup>-1</sup> resolution with each four scans averaged to give a single IR spectrum every 1.15 s.

Carbonyl compounds produced by gas-phase reactions were measured by impinger sampling in a derivatizing solution of 2,4-dinitrophenylhydrazine (DNPH). Hydrazones formed by derivatization were separated and quantitatively measured by HPLC (Hewlett-Packard, Model 1050) using a three-component gradient solvent program, as described previously [8].

OH was generated from the photolysis of methyl nitrite (CH<sub>3</sub>ONO) or nitrous acid (HONO) in the presence of nitric oxide and air [6]. CH<sub>3</sub>ONO was prepared in gram quantities according to procedures outlined by Taylor et al. [9] and retained as a high pressure liquid in a lecture bottle. The generation of OH by this method also produces HCHO as a reaction product. Thus, for mechanistic studies, HCHO yields cannot be determined when methyl nitrite is used as the OH source. The photolysis of HONO, however, can also generate OH directly without forming HCHO, as has been previously described [10]. HONO was prepared according to the procedure of Edney et al. [11] and was introduced directly into the reaction chamber with dry nitrogen.

The following organic reagents were used in the study: TAME, ETBE, methyl acetate, *n*-hexane, *n*-heptane, acetaldehyde, *t*-amyl alcohol, (pure liquids), and *t*-butyl nitrite (90% in *t*-butyl alcohol), which were obtained from Aldrich Chemical Co. With the exception of *t*-butyl nitrite, these compounds had a stated purity of 99+% and were used without further purification. Acetone (99.6%) was obtained from Fisher Scientific and used without further purification. Formic acid (90%) and acetic anhydride (99%) were obtained from Pfaltz and Bauer, Inc. Propane and *n*-butane were obtained as instrument grade gases in lecture bottles (Scott Specialty Gases). Nitric oxide was also obtained in a lecture bottle (National Welders Speciality Gases;

CP grade). Hydrazones used as calibration standards in the carbonyl analysis were synthesized as described earlier [8].

*t*-Amyl formate is not commercially available and had to be synthesized for this study. The method of Stevens and Van Es [12] was used. The procedure was modified to give a ratio of the mixed anhydride (formic-acetic anhydride) to *t*-amyl alcohol of 2:1. The mixture was stirred for more than 24 h and yielded a product of >97% purity as determined by GC/FID. This compound was used in the product studies for calibration solutions and in the OH rate constant measurements.

### *Analytical Procedures*

The procedures employed for performing the kinetics measurements were similar to those described earlier for the reaction of OH with MTBE [10], and ETBE [7]. Reference compounds employed in this study were *n*-hexane, *n*-heptane, ETBE, *n*-butane, and propane. The reactants (e.g., TAME, *n*-hexane, NO, and methyl nitrite) were injected into the dark reaction chamber in a stream of ultra zero air and allowed to stand for 15–30 min. Usually 3 replicate preirradiation analyses were made by injections into the GC to establish baseline concentrations. The relative standard deviation (RSD) for these measurements rarely varied more than  $\pm 2\%$ . Concentrations of the test and reference compounds for all these experiments ranged for 2 to 9 ppmv, NO varied from 5 to 10 ppmv, and methyl nitrite from 10 to 15 ppmv. Mixtures were irradiated for periods of 20–40 s, followed by analysis of the organic components by GC. Generally, three to six irradiation periods were conducted for each experiment. Prior to the rate measurements, each of the reactants were analyzed qualitatively for purity and to check elution time. The analyte and the reference were then irradiated individually in the presence of  $\text{CH}_3\text{ONO}/\text{NO}$  to observe product formation and elution time of those compounds to ensure that the selection of chromatographic conditions which avoid products coeluting with the test and reference compounds.

The general procedures for the experiments to determine the product yields were similar to those of the kinetics experiments. However, the analytical requirements were more stringent for these measurements than for the kinetics measurements, because absolute concentrations of the reacted TAME and its reaction products were required. Most of the experiments employed the photolysis of methyl nitrite as the source of OH, except in the experiments where HCHO yields were measured. Initial reactant conditions and concentrations were the same as those employed in the kinetic experiments except that the reference compound (e.g., *n*-hexane) was omitted.

Identifications of products formed during the irradiation were obtained by GC/FTIR/MS. Full scan electron impact ionization spectra were collected from 35 to 285 mass units. Preliminary identifications were made by searching the Wiley/NBS Mass Spectra Library. The mass spectrometer was tuned each day by using the standard perfluorotributylamine (i.e., FC-43).

IR spectra of the GC effluent were collected concurrently during the GC run from 4000–700  $\text{cm}^{-1}$ . The 8- $\text{cm}^{-1}$  spectra can then be searched and compared against the EPA vapor phase library. Although this library is relatively small compared to the available MS libraries, the library search will often identify the class of the compound, even if the identification is not an exact match. Pure samples of the identified products were then obtained where possible and tested for matching spectra and chromatographic retention time. FTIR performance was checked each day by

checking the centerburst intensity to determine the status of the optical alignment and detector performance using polystyrene. A single beam spectrum was taken to check for possible interferences such as contamination in the lightpipe or poor chamber purging.

Vapor phase calibration standards for the quantitative GC-FID measurements were generated each day by filling Teflon chambers (or bags) with a known volume (100–200 L) of ultrazero air. While each bag was filled, a measured volume (5–10  $\mu\text{L}$ ) of a standard solution was injected into the airstream which swept the volatile liquid components into the bag. For these experiments, all of the detected components were volatile liquids, and at the concentrations used, wall loss of the individual organic compounds in the bag was not observed. The standard solutions were made from dilutions of the various components into methanol. This procedure facilitated the injection of sufficiently large volumes of liquids to produce suitable reproducibility for the day-to-day calibrations. Additionally, the same clean syringe and filler system were used each time, as well as bags that were similar in size of the reaction bags, to minimize systematic errors.

Sample collections on the cryogenic loop were taken for 5–10 min at 20–50  $\text{ml min}^{-1}$  and then flash injected into the GC, as described earlier. Multipoint calibrations over ranges appropriate to the individual components were used. Calibration factors were calculated from peak areas, and all were found to give a linear response with an intercept of zero within experimental uncertainty. Standard gas mixtures were run each day at the beginning and end of each set of experiments to determine calibration factors and check the instrumental performance.

Carbonyl products were collected and measured by an impinger method using DNPH derivatization [8]. Blanks were taken from the prepared irradiation bags just prior to the first irradiation, and additional samples were taken after each subsequent irradiation. Sample volumes were 5 L at 0.5  $\text{L min}^{-1}$  through a calibrated mass flow controller. Detection limits were approximately 0.5 ppbv for each component. DNPH standards were run on the HPLC at the beginning and end of each day of determine calibration and instrument performance.

Kinetics modeling to evaluate the effects of secondary OH reactions with products was performed using a standard chemical kinetics model, in this case CHEMK [13]. The modeling program had been adapted for use on an IBM-compatible personal computer. The TAME-specific mechanism was developed from the results of the product studies.

## Results

The OH rate constants for TAME, TAF, and methyl acetate were determined by a relative rate method. OH radicals generated from the photolysis of methyl nitrite is the primary oxidizing species. During the irradiation, ozone can be produced from the photolysis of  $\text{NO}_2$ . However, the system contains and excess of NO, which reacts with ozone before it can grow to a sufficient abundance to be an important reactant with the test or reference compound. Likewise,  $\text{NO}_3$  radicals, which could be formed from the reaction of ozone with  $\text{NO}_2$ , is reconverted to  $\text{NO}_2$  via reaction with NO. Thus, OH radicals are the only reactive species removing the test and reference compounds from the system.

Since there is no significant loss of the test or reference compounds by wall loss or photolysis, the only significant removal process is by reaction from the OH radical,

given by Reactions (1) and (2).



As has been previously described [3], rate equations for Reactions (1) and (2) can be combined and integrated to yield an expression of the form

$$(I) \quad \frac{\ln([T]_0/[T]_t)}{\ln([R]_0/[R]_t)} = \frac{k_2}{k_1}$$

where  $[R]_0$  and  $[T]_0$  are the initial concentrations of the reference and test compounds, respectively, and  $[R]_t$  and  $[T]_t$  are the concentrations after an arbitrary reaction time,  $t$ . According to this expression,  $k_2/k_1$  is independent of the initial concentration ratios employed. In addition, a plot of  $\ln([T]_0/[T]_t)$  vs.  $\ln([R]_0/[R]_t)$  is linear with a slope equal to  $k_2/k_1$  and an intercept equal to zero. Given a known value for the rate constant of the reference compound, the rate constant for the test compound can be calculated from eq. (II).

$$(II) \quad k_2 = k_1 \times \text{slope}$$

The relative rate of OH decay of TAME was measured in using three types of experimental conditions: (1) experiments where the concentrations of TAME and *n*-hexane were approximately equal; (2) experiments where the concentration of the TAME was significantly higher than the *n*-hexane; and (3) experiments where the concentration of *n*-hexane is significantly higher than the TAME. Under these conditions, if there are any products coeluting with the reactants, the apparent OH rate constant will be significantly different from the other experiments. The data from all three types of these experiments are presented as a single plot in Figure 1. From a least-squares calculation, the slope of the plot (i.e., the relative disappearance of TAME vs. *n*-hexane) is 1.002. (An  $r^2$  correlation coefficient of 0.99 was calculated from the data.) Given the slope and the recommended value of the OH + *n*-hexane rate constant,  $5.61 \times 10^{-12} \text{ cm}^3 \text{ molec}^{-1} \text{ s}^{-1}$  [14], the calculated rate constant for OH + TAME is  $(5.62 \pm 0.07) \times 10^{-12} \text{ cm}^3 \text{ molecules}^{-1} \text{ s}^{-1}$  at the 95% confidence level from the random uncertainty in the slope. This error does not include uncertainties associated with the reference rate constant that was used to convert the relative value to an absolute value. The overall uncertainty of the *n*-hexane rate constant has been conservatively estimated by Atkinson as  $\pm 25\%$  [14].

At the time these data were collected, only one other value for the TAME + OH rate constant ( $7.91 \times 10^{-12} \text{ cm}^3 \text{ molec}^{-1} \text{ s}^{-1}$ ) had been reported [1], and was 40% higher than our measured value. Therefore, to further check our measurement, two other determinations were made using *n*-heptane and ETBE as reference compounds. These data are also presented in Figure 1(a) (circle and square markers, respectively). Using the value of  $(7.15 \times 10^{-12} \text{ cm}^3 \text{ molec}^{-1} \text{ s}^{-1})$  for *n*-heptane [14], a value of  $(5.34 \pm 0.05) \times 10^{-12} \text{ cm}^3 \text{ molec}^{-1} \text{ s}^{-1}$  is computed from a slope of 0.747. Using the value of  $9.73 \times 10^{-12} \text{ cm}^3 \text{ molec}^{-1} \text{ s}^{-1}$  for the OH + ETBE rate constant [6] the slope of 0.585 yields a value of  $(5.69 \pm 0.10) \times 10^{-12} \text{ cm}^3 \text{ molec}^{-1} \text{ s}^{-1}$  for the TAME + OH rate constant. Although the value using *n*-heptane is slightly lower, all of these values are within experimental error and may differ in large part due to uncertainties associated with reference rate constant used.

Of the major products reported, *t*-amyl formate had no previous OH rate constant data reported. In addition, methyl acetate had only two [4,5] previously reported measurements with values differing by a factor of 2 at similar temperatures (ca. 294 K).

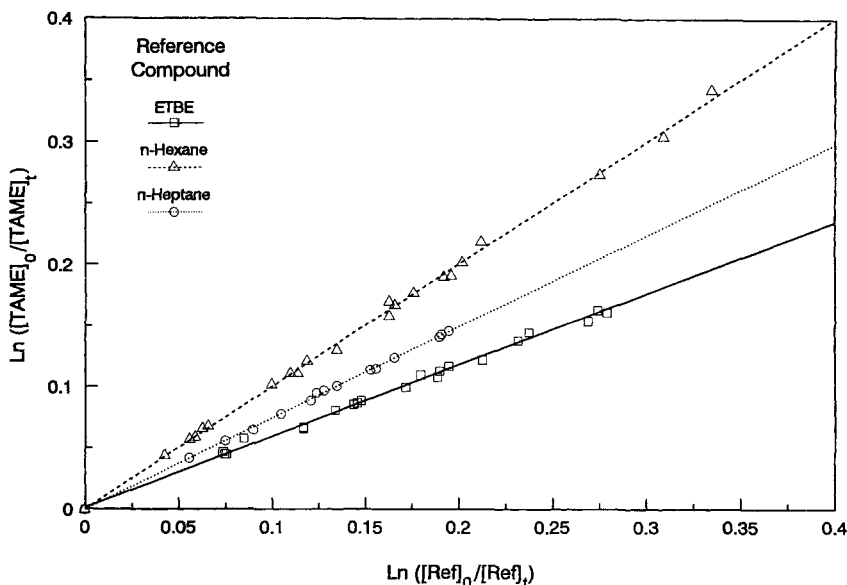


Figure 1. Rate constant for the reaction of OH with TAME by a relative rate technique using three different reference compounds.

Therefore, the OH rate constant was also measured for these two compounds. The measurements were performed in the same manner as those for TAME. For these measurements, propane was used as the reference compound in both cases. The data for these compounds are presented in Figure 2 for measurements made at 298 K. Using a value of  $1.15 \times 10^{-12} \text{ cm}^3 \text{ molec}^{-1} \text{ s}^{-1}$  propane [14] and the experimental slope of 1.52 from Figure 2(a), the OH rate constant for *t*-amyl formate is measured at  $(1.75 \pm 0.05) \times 10^{-12} \text{ cm}^3 \text{ molec}^{-1} \text{ s}^{-1}$ . Using the slope of 0.336, the value for methyl acetate was found to be  $(3.86 \pm 0.16) \times 10^{-13} \text{ cm}^3 \text{ molec}^{-1} \text{ s}^{-1}$ . This value is very similar to that of Wallington et al.  $3.41 \times 10^{-13} \text{ cm}^3 \text{ molec}^{-1} \text{ s}^{-1}$  at 296 K [4] and is substantially higher than the value reported by Campbell and Parkinson of  $1.7 \times 10^{-12} \text{ cm}^3 \text{ molec}^{-1} \text{ s}^{-1}$  (292 K) [5].

Values found for these three compounds have been summarized in Table I. An average value for TAME has been obtained from an average of the data for the use of *n*-hexane and *n*-heptane as reference compounds. The data from the use of ETBE was not used since the data is from a single run and rate constant for OH + ETBE has substantially higher uncertainty than the OH rate constants for the other two reference compounds.

A chromatogram for the formation of the products from the OH-initiated oxidation of TAME (using methyl nitrite) is shown for a typical experiment in Figure 3. A series of experiments are typically performed for increasing extents of reaction. Peak areas are used to determine quantitative values for TAME and each of the products. Quantitative data for the formation of two of the major products from the reaction of TAME + OH are given in Figure 4. In this case, the concentrations of TAF (4(a)) and methyl acetate (4(b)) have been plotted against the amount of TAME reacted to give the yield for the reaction. Similar plots for carbonyl compounds formed in the system are presented in Figures 4(a) and 5 for formaldehyde, acetaldehyde, acetone, and 3-methoxy-3-methyl butanal (MMB). The data for all concentrations include

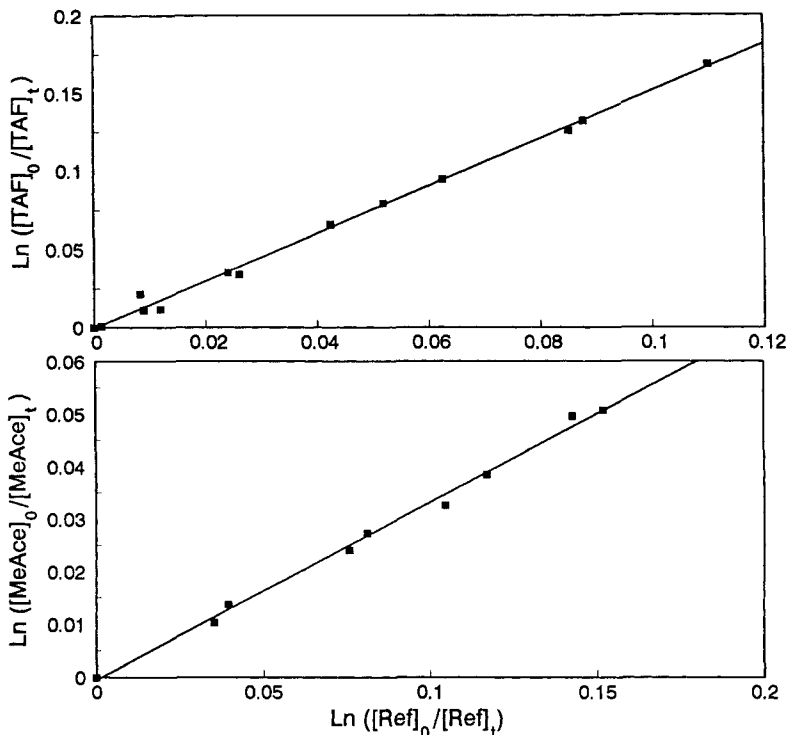


Figure 2. Rate constant for the reaction of OH with (a) *t*-amyl formate and (b) methyl acetate. Propane used as the reference compound for these measurements.

subtractions for preirradiation blanks, and thus the points at the origin represent experimental points. The amount of TAME reacted is determined as the difference between the initial concentration and the concentration after a period of irradiation. For individual experiments, three to five irradiations were performed. The plots are the cumulative results for several experiments combined, including those using either  $\text{CH}_3\text{ONO}$  or  $\text{HONO}$  as the OH source.

The product yields were computed from the slope of an unrestricted linear least-squares fit to the data and are summarized in Table II. In some cases, the yields have been corrected for secondary reaction of the product by OH (see below). In the case of acetaldehyde, the data represent both GC and HPLC data (open boxes and filled boxes,

TABLE I. Rate constants for the reaction of OH with TAME, *t*-amyl formate, and methyl acetate.

Compound	Reference Compound	Rate Constant ( $10^{-12} \text{ cm}^3 \text{ molec}^{-1} \text{ s}^{-1}$ )
<i>t</i> -amyl methyl ether	<i>n</i> -hexane	$5.62 \pm 0.10$
	<i>n</i> -heptane	$5.33 \pm 0.07$
	ethyl <i>t</i> -butyl ether	$5.69 \pm 0.05$
	Average:	$5.48 \pm 0.12^a$
<i>t</i> -amyl formate	propane	$1.75 \pm 0.05$
methyl acetate	propane	$0.386 \pm 0.016$

<sup>a</sup> Average from data for *n*-hexane and *n*-heptane (see text).

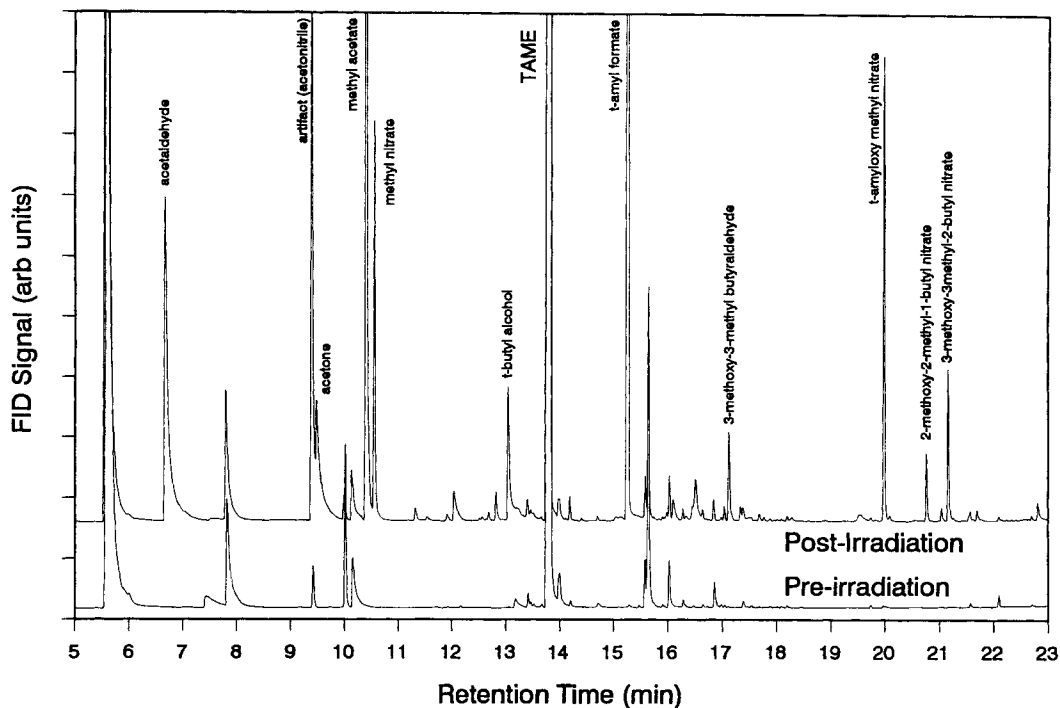


Figure 3. Chromatograms for the reactant mixture before and following irradiation.

respectively). Measurements for TAF and methyl acetate are by GC-FID only while data for formaldehyde are by HPLC only. The data from the plots in Figures 4 and 5 show yields for TAF, methyl acetate, acetaldehyde, and formaldehyde as  $(0.366 \pm 0.049)$ ,  $(0.349 \pm 0.033)$ ,  $(0.338 \pm 0.037)$ , and  $(0.549 \pm 0.076)$ , respectively.

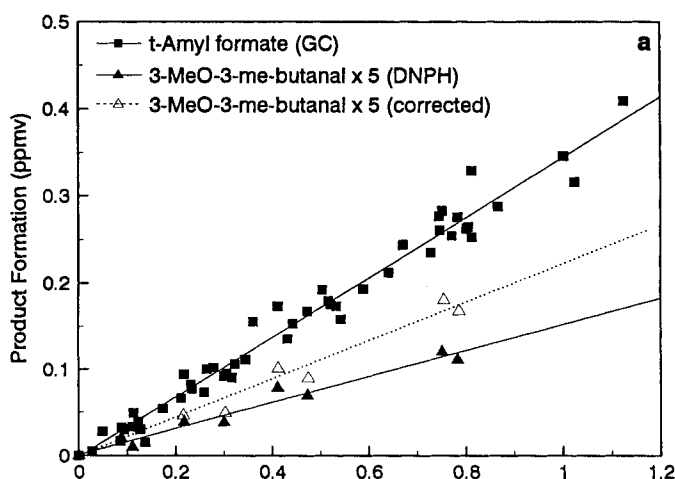


Figure 4. Product formation for products from the reaction of OH + TAME: (a) *t*-amyl formate and 3-methoxy-3-methyl butanal, open triangles, and dotted line show corrections for secondary reaction of MMB with OH and (b) methyl acetate and *t*-amyl alcohol.

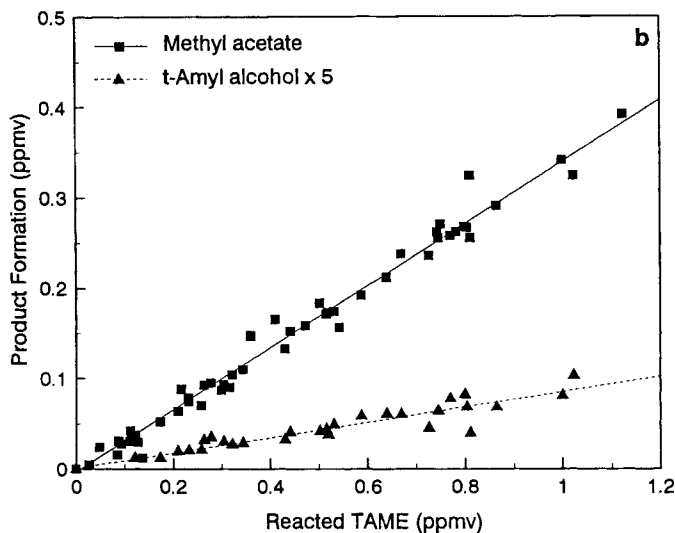


Figure 4. (continued)

Figures 4(a) and 5 also present the quantitative data for two other detected products from the reaction of OH with TAME; acetone and *t*-amyl alcohol. Similar to acetaldehyde, data for acetone (Fig. 5) are represented by GC-FID (open triangles) and HPLC (filled triangles). Data for *t*-amyl alcohol (Figure 4(a)) are from GC-FID measurements only. The slopes from these curves, which are also summarized in Table II, indicate yields of  $(0.036 \pm 0.002)$  and  $(0.026 \pm 0.002)$  for acetone and *t*-amyl alcohol, respectively.

Data for the yields of four tentatively identified minor, but interesting, products are also presented in Figure 6. Three organic nitrates are reproducibly formed as

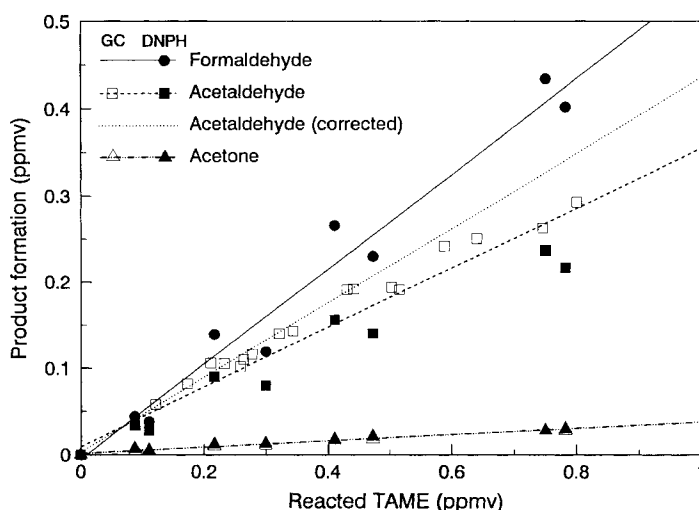


Figure 5. Product formation for carbonyl products from the reaction of OH + TAME. Dotted line shows correction due to secondary reaction of OH + acetaldehyde. Individual corrected points not shown for clarity.

TABLE II. Product yields from the reaction of OH radicals with *t*-amyl methyl ether.

Product Name	Molar yield <sup>a</sup>	$r^2$	% carbon
TAF	$0.366 \pm 0.049$	0.987	36.6
Methyl acetate	$0.349 \pm 0.033$	0.987	17.5
Acetaldehyde <sup>b</sup>	$0.43 \pm 0.043$	0.983	14.3
Formaldehyde	$0.549 \pm 0.076$	0.972	9.2
Acetone	$0.036 \pm 0.002$	0.993	1.8
MMB <sup>b</sup>	$0.044 \pm 0.005$	0.970	4.4
<i>t</i> -Amyl Alcohol	$0.026 \pm 0.002$	0.991	2.2
<i>t</i> -amyloxy methyl nitrate	$0.029 \pm 0.003$	0.984	2.9
3-methoxy-3-methyl-2-butyl nitrate	$0.010 \pm 0.001$	0.978	1.0
2-methoxy-2-methyl-1-butyl nitrate	$0.004 \pm 0.003$	0.992	0.4

<sup>a</sup> Reported errors are the 95% confidence intervals for the slopes of the least-squares analyses.

<sup>b</sup> Reported values for these compounds are corrected for secondary OH reactions. See Figures 4(a) and (5).

addition products (NO + peroxy radical reactions) from the four possible hydrogen atom abstraction sites on the TAME molecule. In some of the experiments where very large samples were collected, a tentative fourth organic nitrate was observed but the yield were so low that no IR spectra and only poor MS data were collected. The three compounds have been identified as: (1) *t*-amyloxy methyl nitrate; (2) 3-methoxy-3-methyl-2-butyl nitrate; and (3) 2-methoxy-2-methyl-1-butyl nitrate. The yields for these compounds are ( $0.026 \pm 0.002$ ), ( $0.010 \pm 0.001$ ), and ( $0.004 \pm 0.0003$ ), respectively. Because no true standards are available, the FID response factor for TAME (which has the same number of carbons) was used to determine the yields for these compounds. The functional group tends to cause a reduced FID carbon response by an estimated 17%. Thus, the reported yields are considered a lower limit to the true value.

A final compound is tentatively identified as 3-methyl-3-methoxy-butanal and was quantified using the HPLC/DNPH derivatization method as shown in Figure 4(a).

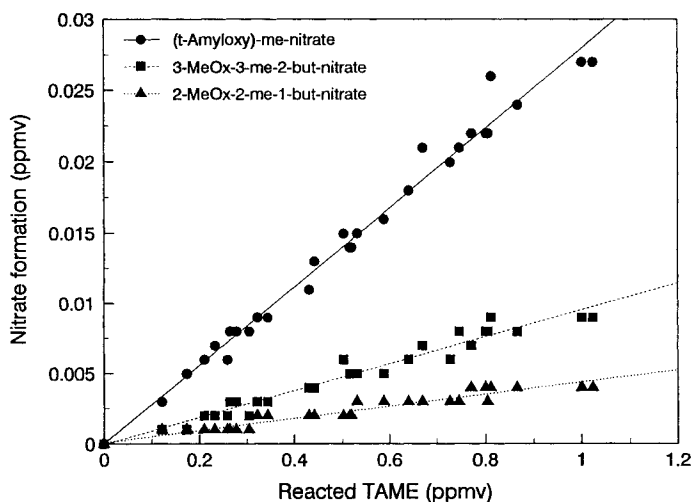


Figure 6. Product formation for organic nitrate products from the reaction of OH + TAME.

Once again, no true standard was available and the response factor for acetone/DNPH derivative was used to quantify the yield. This approach is reasonable as the molar responses for mono-DNPH derivatives are very similar and, thus, the response value is considered to be within  $\pm 15\%$ . The data for these minor components are also summarized in Table II. Mechanisms for the formation of all of these products are discussed below.

Two methods were adopted to evaluate the effect of secondary reactions to the observed yields of products in this system. In the first method the previously described kinetics modeling program [13] was used to solve the coupled differential equations of a mechanism for the photooxidation of TAME in the presence of  $\text{NO}_x$ . The mechanism was written using standard inorganic reactions [15], one and two carbon alkyl, alkyl peroxy, and alkoxy radical reactions, and reactions specific to the oxidation of TAME. The reactions of TAME followed the four mechanistic paths discussed below with the initial branching ratios from the measured product yields (see discussion). From the model results, secondary reactions of OH with the stable ester products of TAME (TAF and methyl acetate) proved to be of negligible importance. The only secondary processes of importance were removal processes for acetaldehyde, formaldehyde, and MMB, since these compounds react rapidly with OH and photolyze. Moreover, the use of the model also gives CO yields, which were not measured during the irradiation, but provide useful information for establishing carbon balances.

Two experiments (using methyl nitrite as the radical source) were modeled for an evaluation of the importance of the secondary reactions of acetaldehyde. The only adjustable parameter used was the photolysis rate of methyl nitrite which was set to give the observed removal of TAME. Rate constants for the organic radicals from TAME were obtained by analogy with other known organic radical reactions. The model determination of acetaldehyde provided agreement that was within 5% of the experimental values. The model calculation was then performed without secondary removal processes for acetaldehyde. These corrected values were then plotted against the removal of TAME. The derived plots indicated that the secondary reaction (OH + acetaldehyde) decreased the primary yield of acetaldehyde by 18.3% at a 10% conversion of TAME. Applying this correction to the measured data (0.338) gives a primary yield of 0.40 for acetaldehyde. This corrected yield compares very favorably with the methyl acetate plus acetone yield of 0.39 seen above. The correction for MMB closely follows that for acetaldehyde. Although the rate constant for OH + MMB has not been measured, it is expected to be fast, probably within a factor of two of that for OH + acetaldehyde. Without an accurate value for the rate constant the correction is difficult to apply, but is estimated to be on the order of 40%. Thus, an overall increase from a 3 to 4.2% yield is obtained for MMB by this approach. However, while the relative increase is high, the effect on the sum of the product yields is minimal.

Similar procedures were adopted for the HONO experiments to determine the magnitude of a correction for formaldehyde. In this case, the model indicated only a marginal increase in HCHO, since the removal of HCHO by OH and photolysis was compensated by formation from the reaction of OH with acetaldehyde. The magnitude of a correction was less than 5% under all experimental conditions used and was substantially less than the precision of the data shown in Figure 5 and Table II. Thus, no correction was provided in this case.

A second approach for determining corrections use a two step mechanism, the formation of a product (P) due to reaction of OH + TAME (e.g., Reaction 2) followed by OH reaction with P. Other processes are assumed to be negligible. This approach,

which has been previously described in detail [16], yields an expression for the correction of the following form,

$$(III) \quad F = \frac{(k_2 - k_P)}{k_2} \times \frac{1 - \frac{[\text{TAME}]_t}{[\text{TAME}]_0}}{\left(\frac{[\text{TAME}]_t}{[\text{TAME}]_0}\right)^{k_P/k_2} - \frac{[\text{TAME}]_t}{[\text{TAME}]_0}}$$

where  $F$  represents the correction,  $k_2$  the rate constant for the reaction of OH with TAME, and  $k_P$  the rate constant for the reaction of OH with P. This expression was applied to the data for MMB and acetaldehyde, the only compounds giving nonnegligible corrections (see below). Application of the equation to the data for MMB and acetaldehyde gave the corrected curves for the yields shown in Figures 4(a) and (5), respectively. Due to the relative simplicity of the approach, these corrected molar yields (acetaldehyde: 0.43; MMB: 0.044) have been incorporated in Table II, but are well within 10% of those given by the model. As noted earlier, the analytical expression was not used to correct HCHO yields, due to a modest formation of HCHO by secondary processes.

### Discussion

The rate constant for the reaction of TAME with OH has been measured in two previous studies. In the earlier work of Wallington et al. [1] using flash photolysis—resonance fluorescence at a series of temperatures between 240 and 440 K, a value of  $7.93 \times 10^{-12} \text{ cm}^3 \text{ molec}^{-1} \text{ s}^{-1}$  at 298 K was obtained. That value is >30% the value initially obtained here  $\{(5.62 \pm 0.07) \times 10^{-12} \text{ cm}^3 \text{ molec}^{-1} \text{ s}^{-1}\}$  using *n*-hexane as the reference compound. Two further measurements were then made using *n*-heptane and then ETBE as the reference compounds. The values obtained using these compounds were in close agreement with our first measurement ( $5.33 \pm 0.05 \times 10^{-12}$  and  $5.69 \pm 0.10 \times 10^{-12} \text{ cm}^3 \text{ molec}^{-1} \text{ s}^{-1}$ , respectively). The study using ETBE as the reference was chosen because the measurements for that compound had been performed in this laboratory and had also used *n*-hexane as the reference compound. The value of  $5.69 \times 10^{-12} \text{ cm}^3 \text{ molec}^{-1} \text{ s}^{-1}$  obtained for TAME vs. ETBE is virtually identical to the value of  $5.62 \times 10^{-12} \text{ cm}^3 \text{ molec}^{-1} \text{ s}^{-1}$  using *n*-hexane and lends strength to the validity of the measurement. The difference between the values obtained using *n*-heptane or *n*-hexane are within the statistical error limits of each other and therefore our recommended value is the mean of the two values, that is,  $5.48 \pm 0.12 \times 10^{-12} \text{ cm}^3 \text{ molec}^{-1} \text{ s}^{-1}$ . It is possible that the measurements differ in the errors associated with the recommended rates of the reference compounds. Subsequent to the completion of these measurements, another study by Wallington et al. [2] reported a value of  $5.5 \times 10^{-12} \text{ cm}^3 \text{ molec}^{-1} \text{ s}^{-1}$  for a flash photolysis measurement, which is essentially identical to the mean value from the present study.

No previous measurements for the reaction of OH with the major product, *t*-amyl formate, have been previously reported. The value reported here is  $(1.75 \pm 0.05) \times 10^{-12} \text{ cm}^3 \text{ molec}^{-1} \text{ s}^{-1}$  using propane as the reference compound using a recommended reaction rate of  $1.15 \times 10^{-12} \text{ cm}^3 \text{ molec}^{-1} \text{ s}^{-1}$  [14]. The product formation rates from TAME (see discussion below) suggests that the reactivity of the alkyl components on each side of the oxygen atom are roughly equal. Thus, the measured value of  $1.75 \times 10^{-12} \text{ cm}^3 \text{ molec}^{-1} \text{ s}^{-1}$  is reasonable since it is on the same order as half the value

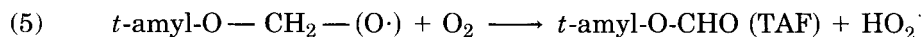
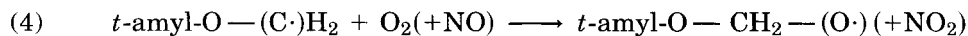
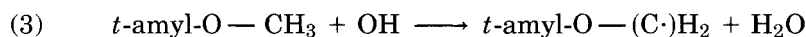
for the reaction of OH + TAME. By analogy with *t*-butyl formate [10], it is expected that virtually all of the H-atom abstraction occurs on the *t*-amyl side of TAF.

Methyl acetate was the other major photooxidation product of TAME for which an OH rate measurement was performed in this study. Two previous measurements have been reported [4,5] with widely differing rates. The value reported by Wallington et al. ( $3.41 \times 10^{-13} \text{ cm}^3 \text{ molec}^{-1} \text{ s}^{-1}$  at 296 K) is in close agreement with the one reported here. The other reported value ( $1.7 \times 10^{-13} \text{ cm}^3 \text{ molec}^{-1} \text{ s}^{-1}$  at 292 K [5]) differs by  $\approx 50\%$ . It is noted in Atkinson [14] that the study by Campbell and Parkinson [5] was systematically low relative to several other studies of the compounds reported therein. This suggests that the value reported here is reasonable and supports the previously reported value by Wallington et al. [4]. Moreover, an examination of the temperature dependence of the data of Wallington et al. [4] suggests that the OH + methyl acetate rate constant could have been systematically low by approximately 15%.

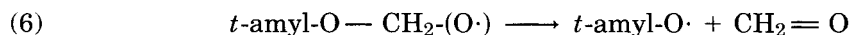
Four major products and six minor products were quantitatively measured during the mechanistic phase of this study. Yields from these products are required to determine the importance of various decomposition pathways. Because TAME emissions are expected to be greatest in urban environments, the distribution of products from the oxidation of TAME was measured in the presence of  $\text{NO}_x$ . Under these conditions, peroxy radicals formed during the oxidation are rapidly converted to alkoxy radicals. It is the disposition of the alkoxy radicals formed in the system that mainly determine the product distribution and branching ratios of possible mechanistic pathways. Alkoxy radicals, in general, can be removed by reaction with  $\text{O}_2$ , decomposition, or isomerization. These processes will be considered for studying the major alkoxy radicals that can be formed in this system, although in most instances reaction by  $\text{O}_2$  and radical decomposition tend to predominate, unless a five or six-membered ring can be formed from the reaction intermediate.

As in the case of MTBE [10], H-atom abstraction is the only viable mechanistic option for the initial attack by OH radicals. Unlike MTBE and ETBE where the *t*-butoxy moiety remains largely intact, large observed yields of methyl acetate relative to TAF indicate that OH attack on both sides of the ether are roughly equivalent. Possible reactions leading to the formation of these two dominant products in the system are expected to be given by the pathways as follows;

#### Path 1



TAF formation takes place by way of Path 1 and is the primary observed product from the reaction of OH with TAME on the methyl side of the ether. The alkoxy radical formed in Reaction (4) may also decompose, however, to yield a *t*-amyloxy radical;

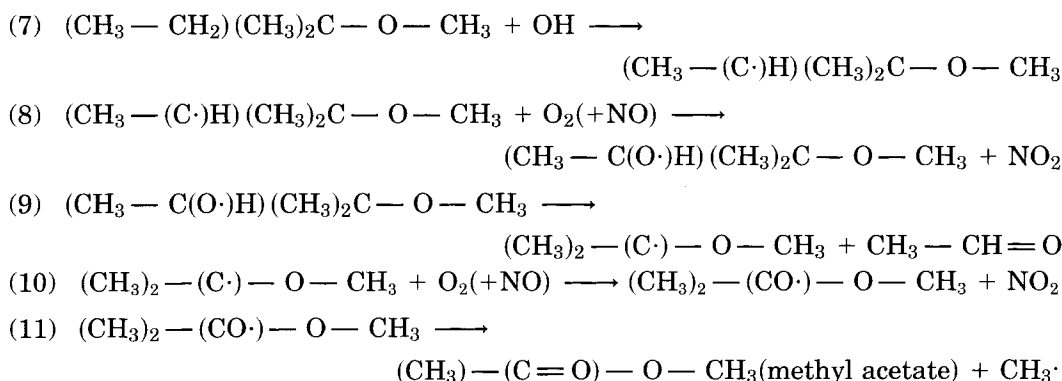


which can subsequently decompose to yield either: (1) acetone and ethyl radicals or (2) methyl ethyl ketone and methyl radicals. A small yield of acetone is observed (0.036) as well as trace of methyl ethyl ketone but the yield is so small (<1%) that it could not be reliably quantified.

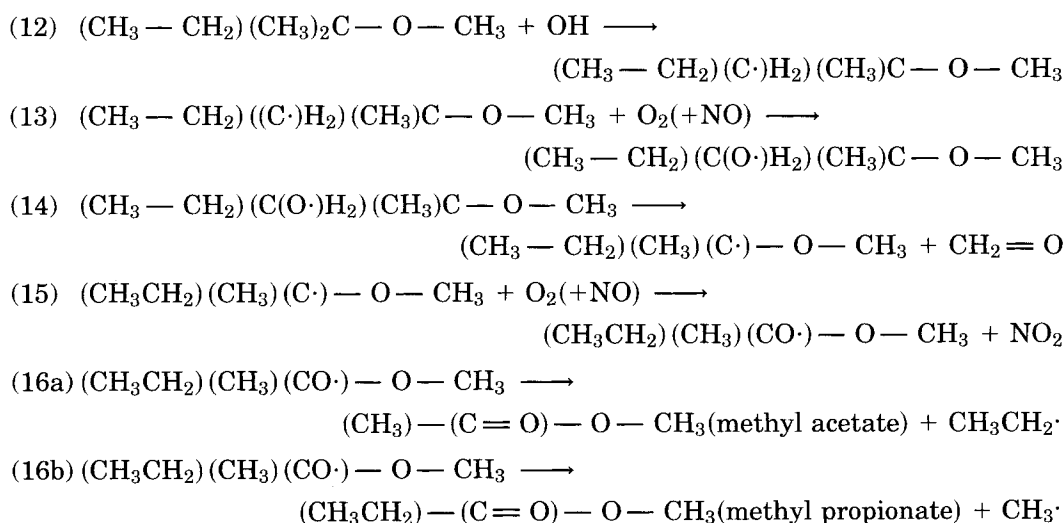
Similar to the formation of *t*-butyl alcohol during the photooxidation of MTBE [10] and ETBE [6], a small yield of *t*-amyl alcohol is detected (0.026). While mechanistically difficult to justify, the product is clearly seen to increase as function of the irradiation time. This is shown in the chromatographic sequence in Figure 3 and can be identified by MS, FT-IR and chromatographic retention times. The tertiary alkoxy radical is apparently sufficiently stable to be able to abstract a hydrogen atom to form the alcohol as an alternate path to decomposing to other products. Unlike MTBE and ETBE where *t*-butyl nitrite was observed [6], we were unable to detect the formation of any *t*-amyl nitrite from this reaction system. Finally, there was no evidence for the formation of products from the alkoxy radicals by a potential isomerization mechanism, by which a six member ring would allow abstraction of a secondary hydrogen. This result is consistent with those from our MTBE study [10], where this possibility was examined in greater detail.

Methyl acetate is the primary product formed from OH attack on the *t*-amyl side the molecule. There are at least three likely paths for this to occur. These are shown in Paths 2, 3, and 4 below;

#### Path 2



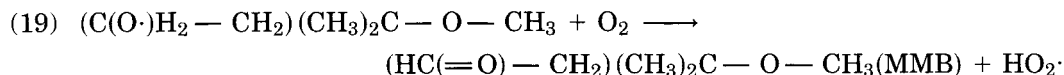
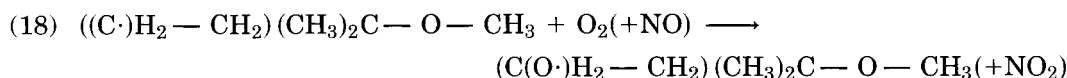
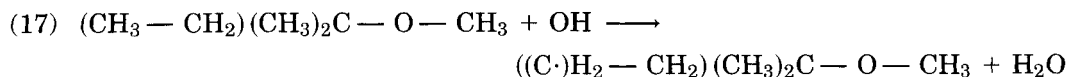
#### Path 3



OH abstraction from the secondary carbon is expected to predominate over abstraction at the primary position [14] and, therefore, Path 2 is expected to predominate over Path 3. The alkoxy radical formed in Reaction (15) can decompose through one of two mechanisms shown in Reactions (16a) and (16b) to yield products. The primary path appears to be by Reaction (16a) to form methyl acetate. However, a trace level of methyl propionate was also detected (<1% yield) but was below levels which could be reliably quantified. If the alkoxy radical in Reaction (8) did not decompose but reacted again with O<sub>2</sub> the product would be 3-methoxy-3-methyl-2-butanone. A small yield of a product initially thought to be this compound was found, however, the mass spectrum proved to be that of another compound. Subsequent analysis has tentatively identified this product as 3-methoxy-3-methyl-butanal which is formed by another pathway.

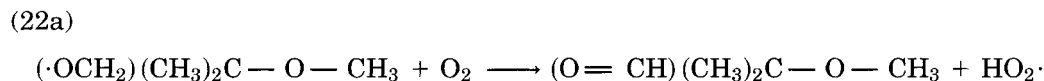
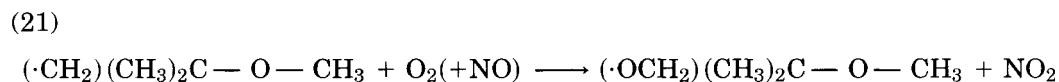
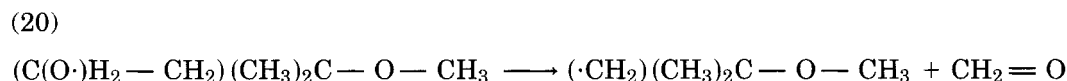
Abstraction at the methyl group on the ethyl side chain can yield several products but only one is obviously distinguishable from the other pathways. This pathway is depicted as follows;

#### Path 4



In this case, MMB would be formed. A small yield of this product was tentatively identified and quantified by HPLC. No standards or spectra were found to substantiate the identification. Also, no FT-IR spectrum could be acquired because of the low yield and an elution time corresponding to a high nitric acid and water background. Therefore, the identification is tentative, although the mass spectrum and the elution time by HPLC are reasonable for this product.

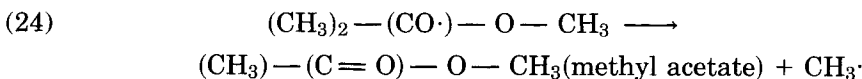
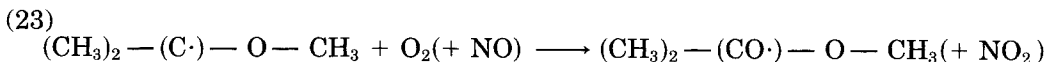
A decomposition mechanism of the radical formed in Reaction (18) could yield the following products;



No evidence for the formation of this product (2-methoxy-2-methyl-propanal) was found from these product studies. This product is the equivalent of H-atom abstraction from the *t*-butyl side of MTBE with subsequent reaction of O<sub>2</sub> and NO. No evidence for its formation was found during the product studies for MTBE [10] either.

If the disposition of the alkoxy radical formed in Reaction (21) proceeds via a decomposition mechanism, then;





the radical formed in Reaction (23) is the same as that formed in Reaction (9) which is further oxidized and subsequently decomposes to yield methyl acetate. The methyl acetate formed here as in Paths 2 and 3 would be indistinguishable from those pathways. Methyl radicals formed in Reactions (11), (16b), and (24) would subsequently yield formaldehyde. The ethyl radical formed in Reaction (16a) can go on to form one acetaldehyde or two moles of formaldehyde. Thus, for methyl acetate from Path 4, three moles of formaldehyde would be formed for each mole of methyl acetate formed. Path 2 would yield one mole of formaldehyde and one mole of acetaldehyde for each mole of methyl acetate while Path 3 would fall in between these depending on the disposition of the ethyl radical. The total acetaldehyde yield should be equal to the sum of the yields from methyl acetate from Path 2 plus the yields from the disposition of the ethyl radicals from the formation of acetone (Path 1, Reaction 6) and methyl acetate (Path 3, Reaction 16a). Disposition of the ethyl radicals could not be measured by any methods used in this study but can be estimated using modeling techniques. The level of acetaldehyde measured ( $0.338 \pm 0.037$ ), however, is consistent with the formation of methyl acetate plus acetone (0.39 v/v) and, depending on the formation pathway of methyl acetate, is within experimental uncertainty. Modeling data predicts this value to be systematically low due to secondary OH reactions and calculates a yield of 0.4 v/v. This yield is completely consistent with the combined yield of 0.39 for methyl acetate plus acetone and, thus, the corrected value is reported in the product table.

At present, there is no way to differentiate between the methyl acetate molecules formed by the different pathways and so no accurate way exists to determine the branching ratio between the abstraction points. Previously published estimation methods such structure-activity relationships (SARs) developed by Atkinson for hydrocarbons and related organic chemicals [17,18] have had considerable difficulty in predicting the decomposition products from branched ethers [19], although published estimates to date have been based on relatively little data for ethers. However, these estimation methods are often used in the absence of other data.

Another possible method to estimate the hydrogen atom abstraction branching ratios on the *t*-amyl side chain is to examine the formation ratios of the organic nitrate products. If one assumes the ratio of the relative formation rate of the nitrate to the formation rate of other products for each of the possible alkoxy radicals formed is equal and the GC sensitivities are equivalent, then the branching ratios for the H atom abstraction can be considered. The possible abstraction points on the *t*-amyl side of the ether are given as follows: (1) six  $\alpha$ -equivalent hydrogens on two equivalent methyl groups attached to the tertiary carbon; (2) two equivalent methylene ( $\beta$ ) hydrogens on the ethyl group; and (3) three equivalent  $\gamma$  hydrogens on the ethyl group. Only two organic nitrate molecules, (A) 3-methoxy-3-methyl-2-butyl nitrate, and (B) 2-methoxy-2-methyl butyl nitrate, are identified with reactions from this side of the molecule. Nitrate A is from the addition following abstraction at the methylene hydrogens (abstraction point 2) while nitrate B is from addition following abstraction at one other six equivalent methyl

hydrogens (abstraction point 1). The formation rate of nitrate A to nitrate B is 2.5:1 while the total methylene to methyl hydrogens is 1:3. Thus, an OH/hydrogen atom abstraction branching ratio of approximately 7.5:1 can be extrapolated from these observations for the methylene ( $\beta$ ) hydrogens to methyl ( $\alpha$ ) hydrogens. While this approach leads only to a coarse estimation, it should be noted that acetaldehyde values generated from the model were very close to those observed.

An examination of Table II shows that  $86.4 \pm 8.6\%$  of the reacted TAME is accounted for by the products TAF, methyl acetate, acetone, MMB, *t*-amyl alcohol, and the three organic nitrates on a molar basis. Because of the asymmetric structure of the TAME, no pair of these products can be formed in a single reaction. The other products reported, acetaldehyde and HCHO, are formed simultaneously with the other products. The major source of uncertainty in these measurements is probably in the determinations of the reacted TAME. The losses for TAME are calculated from the difference of two moderately large numbers. Small systematic uncertainties in the calibration factor of TAME, for example, would influence all of the measurements and could explain the 14% yield of the reacted TAME which was not accounted for.

On a total carbon basis the sum of the product yields in Table II accounts for  $(90.3 \pm 9.0)\%$  of the carbon where the major source of systematic uncertainty is probably in the determinations of HCHO and the disposition of the decomposing alkoxy radical products. From Reactions (9), (13), and (17) which produce the products, methyl acetate, and the disposition of the alkoxy radical in Reaction (6) which produces acetone or *t*-amyl alcohol; HCHO is generated simultaneously. When the measured yields for methyl acetate, acetone, and *t*-amyl alcohol (assuming methyl acetate yields one HCHO and one acetaldehyde) are used, a HCHO yield of 0.41 is calculated. This is approximately 25% lower than the measured yield of 0.549. This may indicate that the alkoxy radicals further decompose to yield HCHO and CO. Because of the high correlation of the results for acetone and acetaldehyde between simultaneous GC and HPLC measurements, the HCHO concentrations (which are based on the same HPLC runs) are considered to have good accuracy. As discussed earlier, corrections for HCHO yields were not adopted for secondary reactions with OH, since the model results indicate that the HCHO removal processes were largely compensated by secondary formation from OH + acetaldehyde and possibly MMB. In any case, HCHO is a compound highly susceptible to secondary formation in these systems, and its primary yield is considered to be the most uncertain of any of the reported yields.

As noted earlier, removal of HCHO from the system occurs by reaction with OH or photolysis. Both processes ultimately generated HO<sub>2</sub> and CO and helps account for a larger percentage of the unknown carbon. The results of modeling the HONO runs indicated approximately a 2% carbon yield can be attributed to CO formation from HCHO removal processes. Since corrections due to secondary OH reactions have already been taken into account, the formation of CO remains as the only known process not included in the calculation of the total yield. The contribution from the calculated CO yield when added to that from Table II would amount to 92% of the total carbon. At present, the identity of the remaining 8% is unknown, although this value represents approximately the same percentage as the estimated uncertainty in the total yield. The major remaining uncertainties include undetected products from possible isomerization reactions. In addition, improved calibration factors for the organic nitrates might also raise the total carbon yields but only by approximately one percent.

## Conclusion

TAME is expected to be predominately removed from the atmosphere by reaction with OH [20]. From this study the rate constant for this reaction determined with a relative rate technique is  $5.48 \times 10^{-12} \text{ cm}^3 \text{ molecule}^{-1} \text{ s}^{-1}$ . If an average diurnal OH concentration of  $1 \times 10^6 \text{ molecule cm}^{-3}$  is assumed, a tropospheric lifetime for TAME of 2.1 days is calculated. Under the conditions of this study in the presence of  $\text{NO}_x$ , ten major products were formed: (1) *t*-amyl formate (0.366); methyl acetate (0.349); acetaldehyde (0.43, corrected); acetone (0.036); formaldehyde (0.549); *t*-amyl alcohol (0.026); 3-methoxy-3-methyl-butanal (0.044, corrected); *t*-amyl methyl nitrate (0.029); 3-methoxy-3-methyl-2-butyl nitrate (0.010); and 2-methoxy-2-methyl butyl nitrate (0.004). The branching ratios for OH abstraction on the methoxy side of TAME to abstraction on the *t*-amyl side were very nearly 1:1. The rate constant for *t*-amyl formate was measured as  $1.75 \times 10^{-12} \text{ cm}^3 \text{ molecule}^{-1} \text{ s}^{-1}$ , which under the conditions noted above corresponds to an atmospheric lifetime of 6.6 days in the absence of atmospheric removal by physical processes. The OH rate constant was also measured for methyl acetate as  $3.85 \times 10^{-13} \text{ cm}^3 \text{ molecule}^{-1} \text{ s}^{-1}$ , which corresponds to an atmospheric lifetime of 30 days due to reaction with OH.

## Acknowledgment

This manuscript presents the results of work performed by ManTech Environmental Technology, Inc. under contract AQ-1-3 to Coordinating Research Council (CRC), Atlanta, Georgia and National Renewable Energy Laboratory (NREL), Golden, Colorado. Mention of trade names or commercial products does not constitute endorsement or recommendation for use.

## Bibliography

- [1] T. J. Wallington, P. Dagaut, R. Liu, and M. J. Kurylo, *Int. J. Chem. Kinet.*, **20**, 541 (1988).
- [2] T. J. Wallington, A. R. Potts, J. M. Andino, W. O. Siegl, Z. Zhang, M. J. Kurylo, and R. E. Huie, *Int. J. Chem. Kinet.*, **25**, 265 (1993).
- [3] J. N. Pitts, Jr., A. M. Winer, S. M. Aschmann, W. P. L. Carter, and R. Atkinson, EPA-600/3-82-038, 1982.
- [4] T. J. Wallington, P. Dagaut, R. Liu, and M. J. Kurylo, *Int. J. Chem. Kinet.*, **20**, 177 (1988).
- [5] I. M. Campbell and P. E. Parkinson, *Chem. Phys. Lett.*, **20**, 385 (1978).
- [6] D. F. Smith, T. E. Kleindienst, E. E. Hudgens, C. D. McIver, and J. J. Bufalini, *Int. J. Chem. Kinet.*, **24**, 199 (1992).
- [7] D. F. Smith, T. E. Kleindienst, E. E. Hudgens, and J. J. Bufalini, *Int. J. Environ. Anal. Chem.*, **54**, 265 (1994).
- [8] D. F. Smith, T. E. Kleindienst, and E. E. Hudgens, *J. Chromatogr.*, **483**, 431 (1989).
- [9] W. D. Taylor, D. Allston, M. J. Moscato, G. D. Fazekas, R. Kozlowski, and G. A. Takacs, *Int. J. Chem. Kinet.*, **12**, 231 (1980).
- [10] D. F. Smith, T. E. Kleindienst, E. E. Hudgens, C. D. McIver, and J. J. Bufalini, *Int. J. Chem. Kinet.*, **23**, 907 (1991).
- [11] E. Edney, S. Mitchell, and J. Bufalini, EPA-600/3-82-092, 1983.
- [12] W. Stevens and A. Van Es, *Recueil*, **83**, 1287 (1964).
- [13] G. Z. Whitten and H. Hogo, EPA-600/3-80-028b, 1980.
- [14] R. Atkinson, *J. Phys. Chem. Ref. Data*, Monograph No. 1, 1990.
- [15] R. Atkinson and A. C. Lloyd, *J. Phys. Chem. Ref. Data*, **13**, 315 (1984).

- [16] R. Atkinson, S. M. Aschmann, W. P. L. Carter, A. M. Winer, and J. N. Pitts, Jr., *J. Phys. Chem.*, **86**, 4563 (1982).
- [17] W. P. L. Carter and R. Atkinson, *J. Atmos. Chem.*, **3**, 377 (1985).
- [18] R. Atkinson, *Atmos. Environ.*, **24A**, 1 (1990).
- [19] R. Atkinson and W. P. L. Carter, *J. Atmos. Chem.*, **13**, 195 (1991).
- [20] R. Atkinson, *Chem. Rev.*, **86**, 69 (1986).

Received February 23, 1994

Accepted August 12, 1994